International Journal of GEOMATE, Feb., 2018 Vol.14, Issue 42, pp.30-36
Geotec., Const. Mat. & Env., DOI: https://doi.org/10.21660/2018.42.7141
ISSN: 2186-2982 (Print), 2186-2990 (Online), Japan

# AN INVESTIGATION ON THE STRENGTH OF AXIALLY LOADED COLD-FORMED STEEL Z-SECTIONS

*James Matthew L. De Jesus and Bernardo A. Lejano[2]

[1,2]Gokongwei College of Engineering, De La Salle University, Philippines

*Corresponding Author, Received: 9 June 2017, Revised:28 July 2017, Accepted: 30 Nov. 2017

**ABSTRACT:** Cold-formed steel (CFS) provides high strength-to-weight ratios that prove efficient in the construction of steel structures. CFS Z-section members exhibit buckling failures that may be difficult to predict due to complexity in geometry. There exists a gap in experimental and computational studies done in the Philippines regarding the structural performance of locally-produced CFS members. The objective of this study is to investigate the load-carrying capacity of Z-section CFS members when subjected to axial compression using experimental and computational methods. The study considers a total of 180 member samples with one section shape, six different lengths and six different thicknesses. Experimentally, the CFS members were subjected to compression loads using a standing steel frame with a hydraulic jack, a load cell and 4 displacement transducers to record the parameters needed for the investigation. High-speed video recordings were used to verify the different failure modes. These are then compared to computational results as per the National Structural Code of the Philippines (NSCP). Furthermore, the study also provides a comparison of experimental and computational results with Finite Element Method (FEM) using ANSYS. The main failure modes were torsional-flexural and distortional buckling. Torsional-flexural buckling was observed in 74.01% of the samples. Although 72.88% of the failure modes were predicted correctly, it was found that the provisions in the NSCP in predicting the strength of the member were relatively high with respect to the experimental and FEM results. This means that the predicted strength was non-conservative. It was also found that a modification factor of 0.52 can be used to achieve similar results between the predicted and actual strength of the member.

*Keywords: Cold-formed Steel, Compression Members, Buckling Failures, Z-section*

## 1. INTRODUCTION

The gap of experimental studies done in the Philippines for CFS may be overlooked by structural designers. The National Structural Code of the Philippines or NSCP (which will also be referred as the Code) stipulates design procedures based on foreign experiments and standards in the application of CFS members in the construction of various types of structures. The use of thinner sections and higher yield strengths can lead to structural design problems [1], [2]. These are due to its complexity that is not routinely encountered by most structural engineers. To allow for safety, the structure must be closely studied in accordance with the Code or other methods such as performance-based analysis.

Currently, there are design provisions for CFS members in the NSCP that can be used by structural designers. It has the capability of computing the compressive strength of Z-section CFS. However, these provisions in the Code were based on design standards formulated in other countries. Although the steel used may be the same, the process of local manufacturing may have slight variation that might affect its performance.

Over the years, the NSCP has been regarded as the sole basis of design of structures all over the Philippines [3]. The provisions in the Code are assumed to be correct and safe. Confidence in safety is achieved when the provisions in the Code are religiously followed. However, the design provisions of Z-section CFS have not been fully verified in the field. Experimental tests are needed to confirm the accuracy of its design. In axial compression, Z-section CFS can be unstable in different failure modes such as local, distortional and flexural or torsional-flexural buckling [4].

For reference, the typical cross-section of a Cold Form Steel Z-section is shown in Fig. 1.

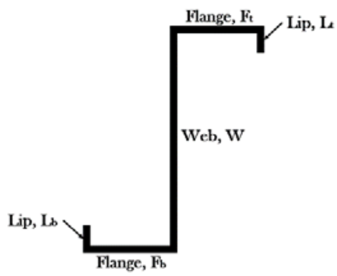


Fig. 1 Cross-section of Z-section CFS

The main objective of this study is to

investigate the load carrying-capacity of Z-shaped Cold Formed Steel when subjected to axial compression. The specific objectives are: (1) to investigate the different buckling modes; (2) to evaluate the axial strength based on the Code and experimental tests; (3) to analyze using Finite Element Method (FEM); and (4) to compare the predictions (Code and FEM) with the experimental results.

## 2. METHODOLOGY

This study focused on experimental and computational methods of research. The experimental method of this study is to conduct compressive tests on Z-section cold-formed steel to acquire its strength and mode of failure. The computational aspect of the study is done by using the formulas recommended by the Code in determining the strength and mode of failure of each member. The critical loads obtained from experiment and calculations are compared to verify the reliability of the Code provisions. Furthermore, these critical loads were then compared to the results of ANSYS Finite Element Method (FEM) analysis.

### 2.1 CFS Z-section specimens

The shape of the section is in the form of a Z and is skew symmetric. The section size conform to the limits for unrestrained Z-sections with simple lip stiffeners stipulated in section 553.4 of the NSCP. The Z-section is with a web and two flanges with simple lip stiffeners as shown in Fig. 1. It is also considered as a point-symmetric section. Based on the availability in the market and to conform to the limits, a 2” x 4” (50mm x 100mm) Z-section CFS member was used in the experiment. That is, 2 inches for the flanges and 4 inches for the web. The code adopted for each member sample type is tabulated in Table 1. There were six thicknesses and six lengths considered in the study. Each type has five test samples, for a total of 180 member samples considered in this study.

Table 1 Code used for the test member sample type

| Code | Length (mm) | Code | Thickness (mm) |
|---|---|---|---|
| 1 | 800 | A | 0.80 |
| 2 | 1100 | B | 1.00 |
| 3 | 1400 | C | 1.20 |
| 4 | 1700 | D | 1.40 |
| 5 | 1800 | E | 1.50 |
| 6 | 2000 | F | 1.80 |

The lengths of the members were based on the experiment done before for C-sections [5]. The thickness of the steel was also dependent on the available thickness that are commercially available. To ensure that calculations were accurate, actual measurements of the dimensions of the samples were taken prior to test of each sample. The measurements were taken using a digital caliper measuring two flanges, two lips, web, thickness and overall height. Each element of the cross-section together with the thickness and length were measured three times at approximately three equidistant sections (e.g. top, middle & bottom). The web height is nominally 100 mm. The flange width is nominally 50 mm. The lip height is nominally 20 mm.

Material properties that were considered to affect the strength and failure modes of the member are the yield strength, fy, and modulus of elasticity, E. These material properties were determined using ASTM E8: Standard Test Methods for Tension Testing of Metallic Materials where strips of metal were cut and tested from the sample population of Z-section CFS. These material properties together with the dimensions parameters were used in determining the nominal strength and effective dimensions of the web, flange and lip elements.

### 2.2 Experimental test set-up

The experimental set-up is illustrated in Fig. 2. The member sample was placed with its transverse axis at a 45-degree angle with respect to the plane of the steel frame. This is to allow space for the placement of the displacement transducer and to ensure that the displacements in the web and flange are recorded.

The member samples were loaded axially in compression by the use of a hydraulic jack. The loading was gradual for all samples. Load cell was placed right below the hydraulic jack to monitor the load that was applied. To simplify the calculation of the axial force, the end conditions were designed to be pin-supported, that is, the supports are not restrained from twisting and bending [5]. To simulate the pin-ended condition of the member, steel end caps were placed in both ends of the member with a 20mm diameter bearing ball attached to provide a ball and socket mechanism for the sample to rotate freely about its ends. The ball was positioned so that the line of action of the force will pass through the centroid of the cross-section of the sample so that the members can be said to be concentrically-loaded.

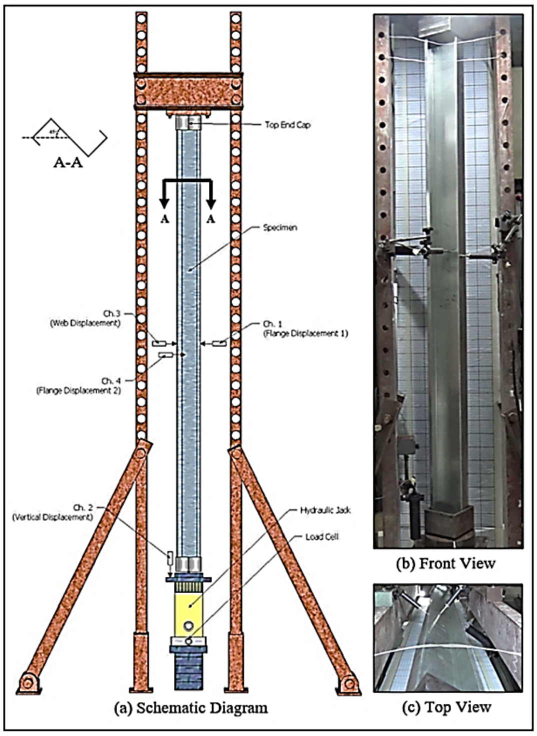


Fig. 2 Experimental set-up

Two displacement transducers were placed in both flanges to record the distortion. Another transducer was also placed in the web to record flexural and/or torsional movement. These three transducers were placed approximately at mid span. Another transducer was placed at the bottom cap to measure the vertical displacement. Data loggers, load cells and transducers were used to measure the experimental data for strength, displacement and deformation to provide accurate results. High-speed cameras were also used to observe the governing failure mode, which is the first buckling failure that occurred. The load, element movements and longitudinal movement were recorded using a data logger which was able to record all four displacements and the load applied to the member.

### 2.3 Failure modes

Evaluation of the failure modes is as important as determining the strength. The modes of failure are mainly of yielding, torsional or torsional-flexural or distortional buckling. The standing steel frame was used with data loggers to determine the movements of the member as it is loaded in compression. Local buckling was usually encountered first. Even if local buckling transpired, it was further loaded to see the buckling mode that the member will exhibit. The different modes of failure are illustrated in Fig. 3. However, the figures just demonstrate the general movements of the elements for each mode. The movement of the elements can either be inward or outward which makes the failure modes more complex. Consequently, a forward or backward movement can also transpire. Furthermore, there exists a local-global interaction in buckling failure modes such that multiple modes can be exhibited by a member sample [6].

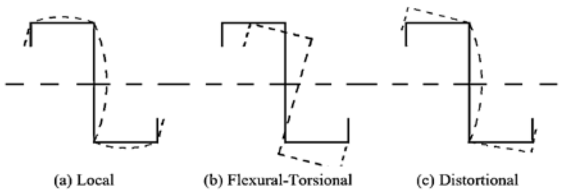


Fig. 3 Section buckling modes of failure

## 3. RESULTS AND DISCUSSION

The calculation of strength depends heavily on the values of the yield strength and modulus of elasticity of Galvanized Iron sheets or G.I. sheets from where the Z-section CFS were made from. Test results indicate an average yield strength obtained was 306.04 which is a typical strength for galvanized iron sheets. Furthermore, the average modulus of elasticity from the test was 23.99 GPa.

### 3.1 Evaluation of strength through experiment

The compressive strengths of the Z-section CFS were evaluated from the 180 samples with varying thickness and length. These strengths will be termed as “experimental strengths”. The experimental strength of each sample was taken as the maximum load recorded. The experimental strength results are summarized in matrix form in Table 2. The first column and first row represents the thicknesses and lengths, respectively. Referring from Table 1, codes A to F represent the thickness, while Codes 1 to 6 represents the length, both in ascending values.

Table 2 Experimental strength results (kN)

| Code | 1 | 2 | 3 | 4 | 5 | 6 |
|---|---|---|---|---|---|---|
| A | 1.64 | 1.37 | 0.93 | 1.19 | 1.20 | 0.79 |
| B | 2.41 | 2.06 | 1.94 | 1.87 | 1.39 | 1.46 |
| C | 3.21 | 2.92 | 2.73 | 2.51 | 2.45 | 2.13 |
| D | 4.96 | 4.33 | 4.17 | 3.31 | 2.84 | 2.77 |
| E | 5.08 | 4.13 | 4.80 | 4.06 | 3.36 | 3.09 |
| F | 8.16 | 6.93 | 5.84 | 5.18 | 4.65 | 3.73 |

As seen in Table 2, the experimental strengths were affected by the thickness and the length. The thicker the member the higher the load it can carry. The longer the member, the lower is the strength.

The length and thickness also influence the buckling mode of failure. Thickness governs the local buckling susceptibility of the individual elements. The length influences the global buckling susceptibility of the member. The values in Table 2 provide a more analytic measure on how much both parameters affect the strength of the member.

The observation of the failure modes was done by identifying the movement both locally and globally. Local, torsional-flexural, and distortional buckling conditions were the main failure modes to be identified. These failure modes can be identified when similar failures are observed as those shown in Fig. 3. As example, Fig. 4 shows torsional-flexural (TF) and distortional buckling (DB). Yielding is not expected to be observed since the GI sheets used in the member are very thin.

Fig. 4 Failure due to torsional-flexural bucking (right) and distortional buckling (left)

### 3.2 Evaluation of strength through computation

The computations of the strength of the members, termed as "computational strength", were done using the formulas and provisions stipulated in the NSCP for the design strength of Cold-Formed Steel compression members. These provisions are summarized in NSCP Sections 552 and 553. The Code considers three main failure modes for CFS Z-section members. These are yielding, torsional-flexural and distortional buckling. The computational strength considered based on the provisions of the code was taken as the lowest load amongst the three failure modes. Although the yielding strength is generally unattainable, it was still computed for comparison with the buckling strength. The computational strength results are summarized in Table 3.

The same influence of thickness and length is observed in the computational strength, that is: the longer the length, the lower the strength; and the thicker the member, the higher the strength. As seen in Table 3, the shortest length of 800 mm and a thickest GI sheet of 1.8 mm resulted to the largest computational strength.

Table 3 Computational strength results (kN)

| Code | 1 | 2 | 3 | 4 | 5 | 6 |
|---|---|---|---|---|---|---|
| A | 4.73 | 4.88 | 4.03 | 3.29 | 3.13 | 2.77 |
| B | 7.42 | 6.53 | 4.79 | 4.01 | 3.90 | 3.46 |
| C | 8.67 | 6.97 | 5.57 | 4.74 | 4.42 | 3.93 |
| D | 11.73 | 8.57 | 6.55 | 5.33 | 4.91 | 4.42 |
| E | 12.50 | 9.25 | 7.04 | 5.72 | 5.15 | 4.69 |
| F | 14.71 | 10.90 | 7.97 | 6.53 | 6.20 | 5.70 |

### 3.3 Evaluation of strength through FEM

"FEM strengths" is the term used for the strength of the members that were obtained using the FEM analysis. There were three general steps in determining the strength of a member. These are generation of the model and setting up of the boundary conditions, solving the model and gathering and analyzing the results [7]. Prior to analysis, an input for the modulus of elasticity, the yield strength, and density of 8027.28 kg/m$^3$ were inputted in the engineering data. The FEM results are summarized in Table 4.

Table 4 FEM strength results (kN)

| Code | 1 | 2 | 3 | 4 | 5 | 6 |
|---|---|---|---|---|---|---|
| A | 0.63 | 0.78 | 0.78 | 0.76 | 0.82 | 0.71 |
| B | 1.54 | 1.58 | 1.25 | 1.47 | 1.58 | 1.58 |
| C | 2.12 | 2.34 | 2.38 | 2.55 | 2.50 | 2.42 |
| D | 3.88 | 4.03 | 3.74 | 3.89 | 3.64 | 3.76 |
| E | 4.57 | 4.93 | 4.51 | 4.83 | 4.57 | 4.41 |
| F | 7.89 | 8.30 | 7.37 | 7.52 | 7.08 | 6.09 |

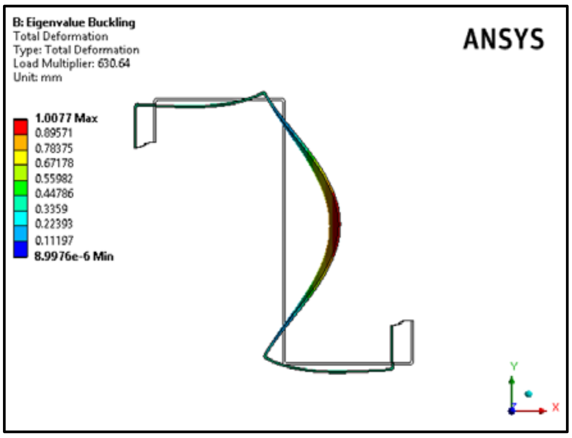


Fig. 5 Cross-section of sample A1 failure using FEM

The goal of using FEM is to verify further the results of the computational and experimental strength evaluations. The strength was analyzed using the Eigenvalue buckling analysis of ANSYS.

A unit axial load was used as the initial load. A sample result of FEM is illustrated in Fig 5. The load multiplier is the strength of sample A1 in Newtons.

### 3.4 Analysis of Strength Evaluation Results

The strength results are compared to one another, as shown in Fig. 6. The diagonal line is the equality line that represents the points at which the computational strength is equal to the experimental strength. Majority of the data points fall below the equality line, indicating over-estimate of the computational strength. The FEM/experimental strength was also plotted and showed good agreement between FEM and experimental strengths. A linear regression was done to show slope for the best-fit line. The FEM strengths show better fit with the experimental results because the $R^2$ value (0.8379) is higher than the $R^2$ value (0.7107) of the computational strengths. Moreover, the y-intercept for the computational/experimental strength plot is approximately equal to zero. This means that a relatively direct relationship can be made between the computational and experimental strength, such that the slope of 0.52 can be used as a factor to make computational strength smaller so as to become almost equal to the actual strength.

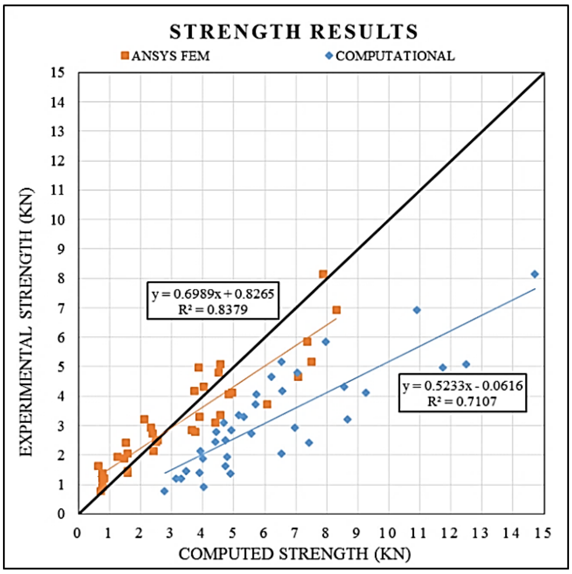


Fig. 6 Comparison of strength results

A comparison between the modes of failures is summarized in Table 5 to check for similarities between the computation and the experimental failure modes. It was calculated that 72.88% of the population are similar. Furthermore, Only 25.99% of the population exhibited distortional buckling failure. Torsional-flexural buckling was the most observed failure, at 74.01%, probably because the Z-section is an open section making it very flexible and weak in resisting to torsion.

The strength ratio is also shown in Table 5. Only the ratio of the experimental strength against the computational strength is shown due to limited space. The values indicated is less than one indicating that the Code does not provide conservative strength predictions. The other strength ratios were also calculated. The experimental against computational strength ratio yielded an average of 0.50 while FEM against computational strength ratio resulted to 0.54. The experimental and FEM agreed well with an average strength ratio of 1.10.

Table 5 Compressive strength results.

| Code | Expt. Mode Fail. | Comp Mode Fail | Ave. Expt. | Ave. Comp | Same ? | Expt/ Compt Ratio |
|---|---|---|---|---|---|---|
| A1 | TF | DB | 1.64 | 4.73 | No | 0.35 |
| B1 | DB | DB | 2.41 | 7.42 | Yes | 0.33 |
| C1 | TF | DB | 3.21 | 8.63 | No | 0.37 |
| D1 | TF | TF | 4.96 | 11.69 | Yes | 0.42 |
| E1 | TF | TF | 5.08 | 12.49 | Yes | 0.41 |
| F1 | TF | TF | 8.16 | 14.71 | Yes | 0.55 |
| A2 | TF | TF | 1.37 | 4.87 | Yes | 0.28 |
| B2 | TF | TF | 2.06 | 6.53 | Yes | 0.32 |
| C2 | TF | TF | 2.92 | 6.97 | Yes | 0.42 |
| D2 | TF | TF | 4.33 | 8.57 | Yes | 0.51 |
| E2 | TF | TF | 4.13 | 9.25 | Yes | 0.45 |
| F2 | DB | TF | 6.93 | 10.90 | No | 0.64 |
| A3 | TF | TF | 0.93 | 4.03 | Yes | 0.23 |
| B3 | TF | TF | 1.94 | 4.79 | Yes | 0.41 |
| C3 | TF | TF | 2.73 | 5.57 | Yes | 0.49 |
| D3 | TF | TF | 4.17 | 6.55 | Yes | 0.64 |
| E3 | TF | TF | 4.80 | 7.04 | Yes | 0.68 |
| F3 | DB | TF | 5.84 | 7.97 | No | 0.73 |
| A4 | DB | TF | 1.19 | 3.29 | No | 0.36 |
| B4 | TF | TF | 1.87 | 4.01 | Yes | 0.47 |
| C4 | DB | TF | 2.51 | 4.74 | No | 0.53 |
| D4 | TF | TF | 3.31 | 5.33 | Yes | 0.62 |
| E4 | DB | TF | 4.06 | 5.72 | No | 0.71 |
| F4 | TF | TF | 5.18 | 6.53 | Yes | 0.79 |
| A5 | TF | TF | 1.20 | 3.13 | Yes | 0.38 |
| B5 | TF | TF | 1.39 | 3.90 | Yes | 0.36 |
| C5 | TF | TF | 2.45 | 4.42 | Yes | 0.55 |
| D5 | DB | TF | 2.84 | 4.91 | No | 0.58 |
| E5 | TF | TF | 3.36 | 5.15 | Yes | 0.65 |
| F5 | TF | TF | 4.65 | 6.20 | Yes | 0.75 |
| A6 | TF | TF | 0.79 | 2.77 | Yes | 0.28 |
| B6 | TF | TF | 1.46 | 3.46 | Yes | 0.42 |
| C6 | TF | TF | 2.13 | 3.93 | Yes | 0.54 |
| D6 | TF | TF | 2.77 | 4.42 | Yes | 0.63 |
| E6 | TF | TF | 3.09 | 4.69 | Yes | 0.66 |
| F6 | TF | TF | 3.73 | 5.70 | Yes | 0.66 |

The FEM results were also compared with the computational and experimental results to verify further the reliability of the results. Statistical analysis using ANOVA was conducted. The p-value for the computational and experimental strength was computed at 4.20x10-7 while that of the FEM and experimental was at 0.67. The results indicate that the FEM and experimental strength had no significant difference while the computational strength had significant difference from both the experimental and FEM strength.

To be able to use the formulas stipulated in the Code that would lead to a safe design, a factor=0.52 must be applied to the computational strength. When this factor is applied, the computational strength would result to a "factored strength" that agrees well with experimental strength as illustrated in Fig. 7. The solid line is the regression line after applying the factor to the original computational strength. On the other hand, the dotted line is the original computational strength.

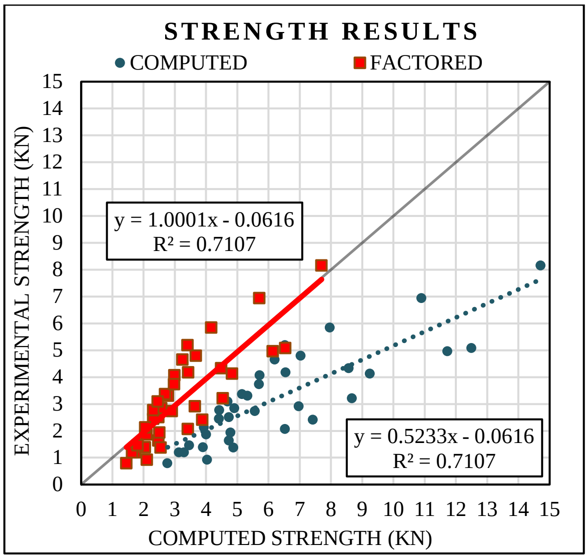


Fig. 7 Strength results with factor = 0.52

## 4. CONCLUSION

The local-global interaction of the buckling failure modes was dependent on the thickness and length of the member. The strength increases as the thickness increases. Consequently, it was found that the longer length contributed to the occurrence of global buckling failures. But, smaller lengths exhibit higher strengths.

The comparison of failure modes shows that 72.88% of the experimental results consistently agree with the computational results. It is concluded that the dominant failure mode was torsional-flexural buckling since 74.01% of the samples experienced this failure.

A comparison between the three strength evaluation methods (experimental, computational, and FEM) is done on the averages of the samples' strengths. The predictions made using the Code formulas were too high such that the average ratio between the experimental and computed strength was only 0.50. Thus it may be concluded that the use of the Code formula for this case (in its present form) may be non-conservative. On the other hand, the average ratio between the experimental and FEM results was 1.10 indicating good agreement.

A modification factor of 0.52 may be used by multiplying it to strength obtained based on the Code. This is to achieve a relatively similar result between the predicted strength and actual strength of the member. This may be done to allow for the use of the provisions of the Code without changing the stipulated equations.

## 5. ACKNOWLEDGEMENTS

Throughout the duration of this study, there are numerous people that the authors would like to thank. Acknowledgement is due to De La Salle University – Manila, Civil Engineering Department for the BSMS program. ERDT is also appreciated for providing the scholarship to one of the authors and for providing a research grant. The authors also acknowledge those who helped in the whole research process, especially in doing the experimental tests.

## 6. REFERENCES

[1] Dubina D, Ungureanu V & Landolfo R, Design of Cold-Formed Steel Structures 1st Edition. Berlin: European Convention for Constructional Steelwork, 2012, ch. 4.

[2] Hancock GJ, "Cold-formed steel structures", Journal of Constructional Steel Research, Vol. 59, April 2003, pp. 473-487.

[3] Association of Structural Engineers of the Philippines, Inc. (ASEP), National Structural Code of the Philippines Volume 1, 6th Edition, 4th Printing. Philippines: Association of Structural Engineers of the Philippines, Inc. (ASEP), 2010, ch. 5

[4] Rondal J, "Cold formed steel members and structures: General Report", Journal of Constructional Steel Research, Vol. 55, 2000, pp. 155-158.

[5] Yu A and Lejano B, "Investigation on the Strength of Cold-Formed Steel C-Section in Compression" in International Conference on Advances on Civil, Structural, Environmental and Bio-Technology CSEB 2014, Kuala Lumpur, Malaysia, 2014.

[6] Batista E, "Local–global buckling interaction procedures for the design of cold-formed columns: Effective width and direct method

integrated approach", Thin-Walled Structures, Vol. 47, April 2009, pp. 1218-1231.
[7] MacDonald M & Kulatunga M. "Finite Element Analysis of Cold–Formed Steel Structural Members with Performations Subjected to Compression Loading", Mechanics and Mechanical Engineering, Vol. 17, May 2013 pp. 127–139.